Exotic $Qq\bar{q}\bar{q}$ states in the chiral quark model

Yuheng Wu,[1,‡] Ye Yan,[2,§] Yue Tan ●,[1,*] Hongxia Huang ●,[2,†] Jialun Ping,[2,‖] and Xinmei Zhu[3,¶]

[1]*Department of Physics, Yancheng Institute of Technology, Yancheng 224000, P. R. China*
[2]*Department of Physics, Nanjing Normal University, Nanjing, Jiangsu 210097, P. R. China*
[3]*Department of Physics, Yangzhou University, Yangzhou 225009, P. R. China*

In the framework of the chiral quark model, we investigate the $Qq\bar{q}\bar{q}$ ($Q = c, b$ and $q = u, d$) tetraquark system with two structures: $Q\bar{q}$-$q\bar{q}$ and Qq-$\bar{q}\bar{q}$. The bound-state calculation shows that for the single channel, there is no evidence for any bound state below the minimum threshold in both $cq\bar{q}\bar{q}$ and $bq\bar{q}\bar{q}$ systems. However, after coupling all channels of two structures, we obtain a bound state below the minimum threshold in the $cq\bar{q}\bar{q}$ system with the energy of 1998 MeV, and the quantum number is $IJ^P = \frac{1}{2}0^+$. Meanwhile, in the $bq\bar{q}\bar{q}$ system, two bound states with energies of 5414 MeV and 5456 MeV are obtained, and the quantum numbers are $IJ^P = \frac{1}{2}0^+$ and $IJ^P = \frac{1}{2}1^+$, respectively. Besides, we also employ the real-scaling method to search for resonance states in the $cq\bar{q}\bar{q}$ and $bq\bar{q}\bar{q}$ systems. Unfortunately, no genuine resonance states were obtained in both systems. We suggest future experiments to search for these three possible bound states.

I. INTRODUCTION

It is full of challenges and opportunities to search for exotic states. So far, many tetraquark and pentaquark states containing heavy quarks have been observed, such as T_{cc} [1], $X(3872)$ [2], $X(4140)$ [3], $P_c(4380)$ [4], and so on. These states allow us to deepen our understanding of nonperturbative quantum chromodynamics (QCD) and hadronic interactions.

In 2016, the D0 Collaboration [5] reported a new state $X(5568)$, which is a good candidate for an exotic tetraquark state because of the four different flavor components (u, d, s, and b). Unfortunately, subsequent experiments from LHCb [6], CDF [7], CMS [8], and ATLAS [9] Collaborations are not confirmed. On the theoretical side, some works support the existence of $X(5568)$ [10–19], while others argue against it [20–25].

Additional fully open flavor tetraquark states are $X_0(2900)$ and $X_1(2900)$ with the quark components

$ud\bar{c}\bar{s}$, which were first reported by LHCb Collaboration in the D^-K^+ invariant mass distributions of the decay process $B^+ \to D^+D^-K^-$ channel [26,27]. The spin-parity of the two states are $J^P = 0^+$ and 1^-, respectively. Their masses and widths are

$$M_{X_0(2900)} = 2866 \pm 7 \text{ MeV},$$
$$\Gamma_{X_0(2900)} = 57 \pm 13 \text{ MeV},$$
$$M_{X_1(2900)} = 2904 \pm 5 \text{ MeV},$$
$$\Gamma_{X_1(2900)} = 110 \pm 12 \text{ MeV}.$$

These two states have attracted a great deal of interest from theorists, and various interpretations have been proposed. Actually, before the experiment, R. Molina, T. Branz, and E. Oset [28] predicted the existence of $\bar{D}^*K^*$ molecular state at the energy around 2900 MeV. After the LHCb observation, they updated it in Ref. [29]. Besides, in the framework of quark delocalization color screening model [30], QCD sum rule [31], quasipotential Bethe–Salpeter equation approach [32], and effective Lagrangian approach [33], the authors explained $X_0(2900)$ as an S-wave $\bar{D}^*K^*$ molecular state. But, in Refs. [34,35], they interpreted the $X_0(2900)$ as an isosinglet compact tetraquark. In Ref. [36], the authors considered the $X_0(2900)$ as a resonance state. For the $X_1(2900)$, in Ref. [37], Huang *et al.* interpret it as a P-wave $D^*\bar{K}^*$ molecule. References [38,39] argue that $X_1(2900)$ is a P-wave diquak-antidiquark state. Moreover, the production and decay properties of these states were investigated.

*Corresponding author: tanyue@ycit.edu.cn
†Corresponding author: hxhuang@njnu.edu.cn
‡191002007@njnu.edu.cn
§221001005@njnu.edu.cn
‖jlping@njnu.edu.cn
¶xmzhu@yzu.edu.cn

In Ref. [40,41], they argue that the isospins of $X_0(2900)$ and $X_1(2900)$ can be investigated by $B \to DX_{0,1}^{\pm,0}$ decays.

Besides, in 2023, LHCb Collaboration announced two new resonant states, $T_{c\bar{s}}^0(2900)$ and $T_{c\bar{s}}^{++}(2900)$, in the decays $B^0 \to \bar{D}^0 D_s^+ \pi^-$ and $B^+ \to D^- D_s^+ \pi^+$ [42]. The minimal quark contents of two new states are $c\bar{s}q\bar{q}(q = u, d)$. The masses and widths of these two resonant states are $2.908 \pm 0.011 \pm 0.020$ GeV and $0.136 \pm 0.023 \pm 0.011$ GeV, respectively. Moreover, the quantum numbers of both states were determined to be $IJ^P = 10^+$. In Ref. [43], utilizing the two-point sum rule method, the authors suggest that $T_{c\bar{s}}^0(2900)$ and $T_{c\bar{s}}^{++}(2900)$ may be modeled as molecules $D_s^{*+}\rho^-$ and $D_s^{*+}\rho^+$, respectively. In a coupled-channel approach, the $T_{c\bar{s}0}(2900)$ were explained as a bound/virtual state [44]. In addition to the molecular states explanation, in Refs. [45,46], the authors argue that the two states are compact tetraquark state. More results and discussions are given in Refs. [47–51].

Inspired by the charm (bottom)-strange tetraquark states, as mentioned above, it is natural to investigate the existence of tetraquarks with one heavy and three light quarks. As is commonly believed, QCD is a fundamental theory of the strong interaction. However, the low energy physics of QCD is much harder to calculate directly from QCD. Various theoretical methods have been proposed to solve this problem, such as Lattice QCD [52], quark delocalization color screening model [53], QCD sum rule [54], and so on.

In addition to these methods, the chiral quark model (ChQM) is also a typical approach, which can well describe hadron-hadron interaction [55] and has been successfully employed to explain some tetraquark [56], pantaquark [57], and hexaquark states [58]. In this work, we use the chiral quark model to systematically investigate the $Qq\bar{q}\bar{q}$ ($Q = c$, b and $q = u$, d) system with the help of Gaussian expansion method (GEM) [59]. GEM is a universal few-body calculation method, which can be used to consider the relative motion between any two quarks, and the Gaussian wave function is used to expand the relative wave function so that the structure of the multiquark system can be obtained. For example, for the tetraquark system in Ref. [60], $X(3872)$ was investigated with the help of GEM and the results shown that $X(3872)$ can be described as a mixing state of the dominant charmonium state (70%) and meson-meson component (30%). For the pentaquark system in Ref. [61], $\Omega(2012)$ was suggested to be a $\Xi^*\bar{K}$ molecular state with quantum number of $IJ^P = 0(\frac{3}{2})^-$ by the help of the GEM. The calculated distances between quarks confirm the molecular nature of the state. For the dibaryon system in Ref. [58], GEM was employed to explore the structure of $d^*(2380)$. The radius of $d^*(2380)$ was around 0.8 fm, which indicated that it is a compact hexaquark state. Besides, Gang Yang and J. Segovia [62] also employed the GEM to investigate $X(6900)$ and interpreted it as a resonance state with $IJ^P = 0^+$ or 2^+. In Ref. [63], with

GEM, the authors calculated the mass shifts, probabilities of the B meson continuum, S-D mixing angles, and strong and dielectric decay widths. Their results show that both S-D mixing and the B meson continuum can contribute to the suppression of the vector meson's dielectric decay width.

The structure of this paper is as follows. Section II gives a brief description of the quark model and wave functions. Section III is devoted to the numerical results and discussions. The summary is shown in the last section.

II. MODEL AND WAVE FUNCTIONS

A. Chiral quark model

In this paper, the chiral quark model (ChQM) has been employed to investigate the $Qq\bar{q}\bar{q}$ ($Q = c$, b and $q = u$, d) tetraquark system. The details of the model can be found in Refs. [64–66]. Here we just present the Hamiltonian of the chiral quark model, $\mathcal{L}$

$$H = \sum_{i=1}^{4} \left(m_i + \frac{p_i^2}{2m_i} \right) - T_{\text{CM}} + \sum_{j>i=1}^{4} (V_{ij}^C + V_{ij}^G + V_{ij}^\chi), \quad (1)$$

where m_i is the constituent mass of quark (antiquark); p_i is the momentum of the quark; T_{CM} is the center-of-mass kinetic energy; V_{ij}^C and V_{ij}^G are the color confinement and one-gluon-exchange interactions; and V_{ij}^χ contains the Goldstone boson and scalar σ exchange potential.

In this work, we focus on the S-wave $Qq\bar{q}\bar{q}$ ($Q = c$, b and $q = u$, d) states, so the tensor force interaction is not included. For the color confinement, the quadratic form is used here,

$$V_{ij}^C = (-a_c r_{ij}^2 - \Delta)\lambda_i^c \cdot \lambda_j^c, \quad (2)$$

where a_c and Δ are model parameters, and λ_i^c is the color Gell–Mann matrices.

One-gluon exchange potential consists of two parts, coulomb and color-magetism interactions,

$$V_{ij}^G = \frac{\alpha_s}{4} \lambda_i^c \cdot \lambda_j^c \left[\frac{1}{r_{ij}} - \frac{2\pi}{3m_i m_j} \sigma_i \cdot \sigma_j \delta(\mathbf{r}_{ij}) \right],$$

$$\delta(\mathbf{r}_{ij}) = \frac{e^{-r_{ij}/r_0(\mu_{ij})}}{4\pi r_{ij} r_0^2(\mu_{ij})}, \qquad r_0(\mu_{ij}) = \frac{r_0}{\mu_{ij}}, \quad (3)$$

where μ_{ij} is the reduced mass between two quarks; σ means the SU(2) Pauli matrices; and α_s is an effective scale-dependent running coupling,

$$\alpha_s(\mu_{ij}) = \frac{\alpha_0}{\ln\left[(\mu_{ij}^2 + \mu_0^2)/\Lambda_0^2\right]}. \quad (4)$$

In the $Qq\bar{q}\bar{q}$ ($Q = c$, b and $q = u$, d) system, there is no Kaon exchange potential due to the absence of s quark.

Therefore, for the meson exchange potentials (V_{ij}^{χ}), the specific forms are as follows:

$$V_{ij}^{\pi} = \frac{g_{ch}^2}{4\pi} \frac{m_{\pi}^2}{12m_i m_j} \frac{\Lambda_{\pi}^2}{\Lambda_{\pi}^2 - m_{\pi}^2} m_{\pi} v_{ij}^{\pi} \sum_{a=1}^{3} \lambda_i^a \lambda_j^a,$$

$$V_{ij}^{\eta} = \frac{g_{ch}^2}{4\pi} \frac{m_{\eta}^2}{12m_i m_j} \frac{\Lambda_{\eta}^2}{\Lambda_{\eta}^2 - m_{\eta}^2} m_{\eta} v_{ij}^{\eta}$$

$$[\lambda_i^8 \lambda_j^8 \cos\theta_P - \lambda_i^0 \lambda_j^0 \sin\theta_P],$$

$$V_{ij}^{\sigma} = -\frac{g_{ch}^2}{4\pi} \frac{\Lambda_{\sigma}^2}{\Lambda_{\sigma}^2 - m_{\sigma}^2} m_{\sigma} \left[Y(m_{\sigma} r_{ij}) - \frac{\Lambda_{\sigma}}{m_{\sigma}} Y(\Lambda_{\sigma} r_{ij}) \right],$$

$$v_{ij}^{\chi} = \left[Y(m_{\chi} r_{ij}) - \frac{\Lambda_{\chi}^3}{m_{\chi}^3} Y(\Lambda_{\chi} r_{ij}) \right] \boldsymbol{\sigma}_i \cdot \boldsymbol{\sigma}_j,$$

$$\chi = \pi, \quad \eta, \quad Y(x) = e^{-x}/x, \tag{5}$$

where $Y(x) = e^{-x}/x$ is the standard Yukawa function; m_{π} and m_{η} are the masses of $SU(3)$ Goldstone bosons, taken to be their experimental values; m_{σ} is determined by the PCAC (partial conservation of axial-vector current) relation $m_{\sigma}^2 \approx m_{\pi}^2 + 4m_{u,d}^2$; Λ_{χ} and Λ_{σ} represent the cutoff; and g_{ch} is the coupling constant for chiral field, which is determined from the $NN\pi$ coupling constant through

$$\frac{g_{ch}^2}{4\pi} = \left(\frac{3}{5}\right)^2 \frac{g_{\pi NN}^2}{4\pi} \frac{m_{u,d}^2}{m_N^2}. \tag{6}$$

It is well known that pion exchange would lead to a delta term in the spatial potential. When a pointlike particle is considered, the delta term is indeed present in the pion exchange potential. However, the calculation of the tetraquark system cannot be considered as a pointlike particle. In Ref. [67], the authors give the delta term expression of the pion exchange potential as:

$$\delta_{\pi}(b) = -4 \frac{\Lambda^2}{\Lambda^2 - \mu^2} \frac{f_{\pi q}^2}{4\pi\mu^2} \sqrt{\frac{2}{\pi}} \frac{1}{b}$$

$$\times \left\{ \mu^2 \left[1 - \sqrt{\pi}\left(\frac{\mu b}{\sqrt{2}}\right) e^{\mu^2 b^2/2} erfc\left(\frac{\mu b}{\sqrt{2}}\right) \right] \right.$$

$$\left. - (\mu \leftrightarrow \Lambda) \right\}. \tag{7}$$

In our work, we can obtain an expression similar to Eq. (7) when we solve the standard Yukawa function.

For the σ meson, there is currently a debate. For several decades, researchers have been studying the properties of the σ meson. Calculations in the GI model [68] suggest that the mass of the 0^{++} $q\bar{q}$ state is much more than the mass reported from experiment. By employing two valence quarks and two antiquarks, Jaffe was able to effectively create a color-neutral resonance and shows that this configuration can result in a nonet of light scalar-isoscalar

mesons [69]. Recently, a drawback has been found in the pure tetraquark picture, because Weinberg has shown that the tetraquark is as narrow as traditional mesons in the $N_c \to$ limit. Currently, there is a theoretical tendency to consider the σ meson as a mixed state of two quarks and four quarks, seen in the review [70], similar to the mixed state of $X(3872)$ (composed of $c\bar{c} + D\bar{D}^*$) [60]. In addition, there is a view that σ is generated by $\pi\pi$ interaction. Based on this picture, the coupling constants of σ and other hadrons have been calculated in the framework of the one-boson-exchange model [71]. In this work, the resulting effective coupling constant can be used to describe the interactions between light hadrons and other hadrons via σ exchange.

At the early stage, nucleon-nucleon interactions and nucleon-nucleon scattering have been investigated by using constituent quark model. In Ref. [72], the authors found when only the exchange of one-gluon and the confinement potential are considered, the quark-cluster model lacks of enough medium- and long-range force to produce the nucleon-nucleon interaction. The long-range part can be solved by introducing a direct coupling between quarks and pions, but for the medium-range part, one usually considers a sigmalike exchange potential between the two interacting baryons. This is a phenomenological approach.

In 1994, Zong-ye Zhang et al. [73] studied the baryon-baryon interaction in a modified model, in which besides the confinement and one-gluon exchange potentials, the pseudoscalar mesons and sigma meson exchanges were included as the nonperturbative effect. Using this interaction they studied the binding energy of the deuteron, the nucleon-nucleon scattering phase shifts and the hyperon-nucleon cross section, and the results were reasonably consistent with experiments. Besides, in Ref. [74], Dai et al. showed that the vector meson exchange potential could substitute one-gluon exchange potential to explain repulsive core of the nucleon-nucleon interaction. Therefore, the role of the vector meson exchange might be replaced by one-gluon exchange interaction. So, here we have not added the vector meson exchange potential to avoid double counting.

The other symbols in the above expressions have their usual meanings. All model parameters, which are determined by fitting the meson spectrum, are from the work [75], as shown in Table I.

B. The wave function of the $Qq\bar{q}\bar{q}$ system

For the $Qq\bar{q}\bar{q}$ system, meson-meson and diquark-antidiquark (replaced by $Q\bar{q}$-$q\bar{q}$ and Qq-$\bar{q}\bar{q}$ after) structures are considered, as shown in Fig. 1. Figure 1(a) represents the $Q\bar{q}$-$q\bar{q}$ structure and (b) means the Qq-$\bar{q}\bar{q}$ structure. The wave function of both structures consist of four parts: orbit, spin, flavor, and color wave functions. In addition, the wave function of each part is constructed by coupling two subcluster wave functions. Thus, the wave function for

TABLE I. Quark model parameters ($m_\pi = 0.7$, $m_\sigma = 3.42$, $m_\eta = 2.77$ (unit: fm^{-1})).

Quark masses	$m_u = m_d$ (MeV)	313
	m_c (MeV)	1728
	m_b (MeV)	5112
Goldstone bosons	$\Lambda_\pi = \Lambda_\sigma$(fm^{-1})	4.2
	Λ_η(fm^{-1})	5.2
	$g_{ch}^2/(4\pi)$	0.54
	$\theta_p(°)$	−15
Confinement	a_c (MeV · fm^{-2})	101
	Δ (MeV)	−78.3
OGE	α_0	3.67
	Λ_0(fm^{-1})	0.033
	μ_0 (MeV)	36.976
	$\hat{r}_0$ (MeV)	28.17

each channel will be the tensor product of orbit ($|R_i\rangle$), spin ($|S_j\rangle$), color ($|C_k\rangle$), and flavor ($|F_l\rangle$) components,

$$|ijkl\rangle = \mathcal{A}[|R_i\rangle \otimes |S_j\rangle \otimes |C_k\rangle \otimes |F_l\rangle], \tag{8}$$

where $\mathcal{A}$ is the antisymmetrization operator. For the $Qq\bar{q}\bar{q}$ system, $\mathcal{A} = 1 - P_{24}$.

For the orbit wave function, the total wave function consists of two subcluster orbit wave functions and the relative motion wave function between two subclusters. Since we are interested in the S-wave system, we put all the orbital angular momenta equal to zero. Here, the magnetic quantum number ($M = 0$) is omitted.

$$|R_1\rangle = [[\Psi_{l_1}(\boldsymbol{r}_{12})\Psi_{l_2}(\boldsymbol{r}_{34})]_{l_{12}}\Psi_{L_r}(\boldsymbol{r}_{1234})]_{LM_L},$$
$$|R_2\rangle = [[\Psi_{l_1}(\boldsymbol{r}_{13})\Psi_{l_2}(\boldsymbol{r}_{24})]_{l_{12}}\Psi_{L_r}(\boldsymbol{r}_{1324})]_{LM_L}, \tag{9}$$

where the bracket "[ ]" indicates angular momentum coupling, and the "L" means total orbit angular momentum coupled by "L_r," relative motion angular momentum, and "l_{12}" coupled by "l_1" and "l_2," subcluster angular momenta. In addition, we use "$|R_1\rangle$" to denote meson-meson structure while "$|R_2\rangle$" denotes diquark-antidiquark
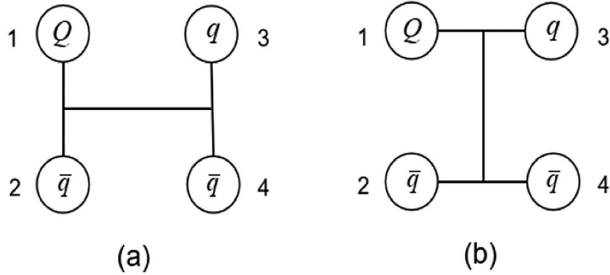
FIG. 1. Configurations of $Qq\bar{q}\bar{q}$ ($Q = c, b$) tetraquarks.

structure. In Gaussian expansion method (GEM), the radial part of spatial wave function is expanded by Gaussians [59]:

$$R(\boldsymbol{r}) = \sum_{n=1}^{n_{\max}} c_n \psi_{nlm}^G(\boldsymbol{r}), \tag{10a}$$

$$\psi_{nlm}^G(\boldsymbol{r}) = N_{nl}r^l e^{-\nu_n r^2} Y_{lm}(\hat{\boldsymbol{r}}), \tag{10b}$$

where N_{nl} are normalization constants,

$$N_{nl} = \left[\frac{2^{l+2}(2\nu_n)^{l+\frac{3}{2}}}{\sqrt{\pi}(2l+1)}\right]^{\frac{1}{2}}. \tag{11}$$

c_n are the variational parameters, which are determined dynamically. The Gaussian size parameters are chosen according to the following geometric progression

$$\nu_n = \frac{1}{r_n^2}, \qquad r_n = r_1 a^{n-1}, \qquad a = \left(\frac{r_{n_{\max}}}{r_1}\right)^{\frac{1}{n_{\max}-1}}. \tag{12}$$

This procedure enables optimization of the ranges using just a small number of Gaussians.

For the spin wave functions, there is no difference between quark and antiquark. The meson-meson structure has the same total spin as the diquark-antidiquark structure. The spin wave functions of the cluster are shown below.

$$\chi_{11}^\sigma = \alpha\alpha, \qquad \chi_{10}^\sigma = \frac{1}{\sqrt{2}}(\alpha\beta + \beta\alpha),$$

$$\chi_{1-1}^\sigma = \beta\beta, \qquad \chi_{00}^\sigma = \frac{1}{\sqrt{2}}(\alpha\beta - \beta\alpha). \tag{13}$$

According to the Clebsch–Gordan coefficient table, total spin wave function can be written below.

$$|S_1\rangle = \chi_0^{\sigma 1} = \chi_{00}^\sigma \chi_{00}^\sigma,$$

$$|S_2\rangle = \chi_0^{\sigma 2} = \sqrt{\frac{1}{3}}(\chi_{11}^\sigma \chi_{1-1}^\sigma - \chi_{10}^\sigma \chi_{10}^\sigma + \chi_{1-1}^\sigma \chi_{11}^\sigma),$$

$$|S_3\rangle = \chi_1^{\sigma 1} = \chi_{00}^\sigma \chi_{11}^\sigma,$$

$$|S_4\rangle = \chi_1^{\sigma 2} = \chi_{11}^\sigma \chi_{00}^\sigma,$$

$$|S_5\rangle = \chi_1^{\sigma 3} = \frac{1}{\sqrt{2}}(\chi_{11}^\sigma \chi_{10}^\sigma - \chi_{10}^\sigma \chi_{11}^\sigma),$$

$$|S_6\rangle = \chi_2^{\sigma 1} = \chi_{11}^\sigma \chi_{11}^\sigma, \tag{14}$$

where the subscript of "$\chi_S^{\sigma i}$" denotes total spin of the tretraquark, and the superscript is the index of the spin function with fixed S.

The flavor wave functions of the subclusters for two structures are shown below,

$$\chi_{\frac{1}{2}\frac{1}{2}}^{fm} = Q\bar{d}, \quad \chi_{\frac{1}{2}-\frac{1}{2}}^{fm} = -Q\bar{u}, \quad \chi_{11}^{fm} = u\bar{d},$$

$$\chi_{10}^{fm} = \frac{1}{\sqrt{2}}(-u\bar{u} + d\bar{d}), \quad \chi_{00}^{fm} = \frac{1}{\sqrt{2}}(-u\bar{u} - d\bar{d}), \quad (15)$$

$$\chi_{\frac{1}{2}\frac{1}{2}}^{fd} = Qd, \quad \chi_{\frac{1}{2}-\frac{1}{2}}^{fd} = Qu, \quad \chi_{11}^{fd} = \bar{d}\,\bar{d},$$

$$\chi_{00}^{fd} = \frac{1}{\sqrt{2}}(\bar{u}\,\bar{d} - \bar{d}\,\bar{u}), \quad \chi_{10}^{fd} = -\frac{1}{\sqrt{2}}(\bar{u}\,\bar{d} + \bar{d}\,\bar{u}), \quad (16)$$

where $Q = c$, b and the subscripts of $\chi_I^{fm(d)}$ are the isospin and its third component. The total flavor wave functions can be written as,

$$|F_1\rangle = \chi_{\frac{1}{2}}^{fm} = \sqrt{\frac{2}{3}}\chi_{11}^{fm}\chi_{\frac{1}{2}-\frac{1}{2}}^{fm} - \sqrt{\frac{1}{3}}\chi_{10}^{fm}\chi_{\frac{1}{2}\frac{1}{2}}^{fm},$$

$$|F_2\rangle = \chi_{\frac{1}{2}}^{fm} = \chi_{\frac{1}{2}\frac{1}{2}}^{fm}\chi_{00}^{fm},$$

$$|F_3\rangle = \chi_{\frac{3}{2}}^{fm} = \chi_{11}^{fm}\chi_{\frac{1}{2}\frac{1}{2}}^{fm},$$

$$|F_4\rangle = \chi_{\frac{1}{2}}^{fd} = \sqrt{\frac{2}{3}}\chi_{11}^{fd}\chi_{\frac{1}{2}-\frac{1}{2}}^{fd} - \sqrt{\frac{1}{3}}\chi_{10}^{fd}\chi_{\frac{1}{2}\frac{1}{2}}^{fd},$$

$$|F_5\rangle = \chi_{\frac{1}{2}}^{fd} = \chi_{\frac{1}{2}\frac{1}{2}}^{fd}\chi_{00}^{fd},$$

$$|F_6\rangle = \chi_{\frac{3}{2}}^{fd} = \chi_{11}^{fd}\chi_{\frac{1}{2}\frac{1}{2}}^{fd}, \quad (17)$$

where the subscript of $\chi_I^{fm(d)}$ is the total isospin.

The colorless tetraquark system has four color structures, including $1 \otimes 1$, $8 \otimes 8$, $\bar{3} \otimes 3$, and $6 \otimes \bar{6}$,

$$|C_1\rangle = \chi_{1\otimes 1}^{m1} = \frac{1}{\sqrt{9}}(\bar{r}r\bar{r}r + \bar{r}r\bar{g}g + \bar{r}r\bar{b}b + \bar{g}g\bar{r}r + \bar{g}g\bar{g}g$$
$$+ \bar{g}g\bar{b}b + \bar{b}b\bar{r}r + \bar{b}b\bar{g}g + \bar{b}b\bar{b}b),$$

$$|C_2\rangle = \chi_{8\otimes 8}^{m2} = \frac{\sqrt{2}}{12}(3\bar{b}r\bar{r}b + 3\bar{g}r\bar{r}g + 3\bar{b}g\bar{g}b + 3\bar{g}b\bar{b}g$$
$$+ 3\bar{r}g\bar{g}r + 3\bar{r}b\bar{b}r + 2\bar{r}r\bar{r}r + 2\bar{g}g\bar{g}g + 2\bar{b}b\bar{b}b - \bar{r}r\bar{g}g$$
$$- \bar{g}g\bar{r}r - \bar{b}b\bar{g}g - \bar{b}b\bar{r}r - \bar{g}g\bar{b}b - \bar{r}r\bar{b}b),$$

$$|C_3\rangle = \chi_{\bar{3}\otimes 3}^{d1} = \frac{\sqrt{3}}{6}(rg\bar{r}\,\bar{g} - rg\bar{g}\,\bar{r} + gr\bar{g}\,\bar{r} - gr\bar{r}\,\bar{g} + rb\bar{r}\,\bar{b},$$
$$- rb\bar{b}\,\bar{r} + br\bar{b}\,\bar{r} - br\bar{r}\,\bar{b} + gb\bar{g}\,\bar{b} - gb\bar{b}\,\bar{g}$$
$$+ bg\bar{b}\,\bar{g} - bg\bar{g}\,\bar{b}),$$

$$|C_4\rangle = \chi_{6\otimes\bar{6}}^{d2} = \frac{\sqrt{6}}{12}(2rr\bar{r}\,\bar{r} + 2gg\bar{g}\,\bar{g} + 2bb\bar{b}\,\bar{b} + rg\bar{r}\,\bar{g}$$
$$+ rg\bar{g}\,\bar{r} + gr\bar{g}\,\bar{r} + gr\bar{r}\,\bar{g} + rb\bar{r}\,\bar{b} + rb\bar{b}\,\bar{r} + br\bar{b}\,\bar{r}$$
$$+ br\bar{r}\,\bar{b} + gb\bar{g}\,\bar{b} + gb\bar{b}\,\bar{g} + bg\bar{b}\,\bar{g} + bg\bar{g}\,\bar{b}), \quad (18)$$

where $|C_1\rangle$, $|C_2\rangle$, $|C_3\rangle$, and $|C_4\rangle$ represent color singlet-singlet ($1 \otimes 1$), color octet-octet ($8 \otimes 8$), color triplet-antitriplet ($\bar{3} \otimes 3$), and color sextet-antisextet ($6 \otimes \bar{6}$) wave functions, respectively. The state with color wave function

$|C_1\rangle$ is color-singlet channel, and the one with $|C_2\rangle$, $|C_3\rangle$, or $|C_4\rangle$ is hidden-color channel.

Finally, we can acquire the total wave functions by substituting the wave functions of the orbital, the spin, the flavor, and the color parts into Eq. (8) according to the definite quantum number of the system.

III. RESULT AND DISCUSSION

The S-wave low-lying states of $Qq\bar{q}\,\bar{q}$ ($Q = c$, b and $q = u$, d) tetraquark systems are systematically investigated with both $Q\bar{q}\text{-}q\bar{q}$ and $Qq\text{-}\bar{q}\,\bar{q}$ configurations in the framework of ChQM. The channel coupling of the two configurations are considered. Since we are focused on the S-wave states, the orbital angular momentum is set to be zero. The spin quantum number of the $Qq\bar{q}\,\bar{q}$ system can be 0,1, and 2, so the total angular momentum can be $J = 0$, 1, and 2 for this system. The isospin of the Q (c, b) quark is zero. It follows that the isospin of the $Q\bar{q}(Qq)$ can only be $\frac{1}{2}$, while the isospin of $q\bar{q}(\bar{q}\,\bar{q})$ can be 0 or 1. In this way, the quantum number of the $Qq\bar{q}\,\bar{q}$ tetraquark system can be $IJ^P = \frac{1}{2}0^+, \frac{1}{2}1^+, \frac{1}{2}2^+, \frac{3}{2}0^+, \frac{3}{2}1^+, \frac{3}{2}2^+$.

In the $Qq\bar{q}\,\bar{q}$ system, we call a color-single state as the scattering state if its energy is above the corresponding threshold. In contrast, a bound state is available if its energy is below the corresponding threshold. For hidden-color channels, which are bound due to their internal color interactions, they can decay to the corresponding color-singlet threshold, possibly forming a color structure resonance state. Besides, if the energy of the hidden-color channel is below the minimum color-singlet threshold, it is also a bound state.

A. $cq\bar{q}\,\bar{q}$ system

The energies of the $cq\bar{q}\,\bar{q}$ tetraquark systems for both $c\bar{q}\text{-}q\bar{q}$ and $cq\text{-}\bar{q}\,\bar{q}$ structures, as well as the channel coupling of these two structures are listed in Table II.

For the $IJ^P = \frac{1}{2}0^+$ system, there are eight channels (four color singlet-singlet channels and four color octet-octet channels) of $c\bar{q} - q\bar{q}$ structure and four channels (two color triplet-antitriplet channels and two sextet-antisextet channels) of $cq\text{-}\bar{q}\,\bar{q}$ structure. From Table II we can see that the energy of each single channel is above the corresponding theoretical threshold. When we couple eight channels of $c\bar{q}\text{-}q\bar{q}$ structure, the lowest energy of the system is still above the lowest threshold of the channel πD.

For the $cq\text{-}\bar{q}\,\bar{q}$ structure, the energy of each channel is several hundred MeVs higher than the minimum color single channel (πD). By coupling with these four channels, the energy of 2437 MeV is obtained, which is still much higher than the minimum threshold (πD). These results are qualitatively consistent with those in Ref. [76], the work of which study the $nn\bar{n}\,\bar{c}$ (n = u, d) system with the $nn\text{-}\bar{n}\,\bar{c}$ structure in the framework of an extended relativized quark model. However, quantitatively, the energy obtained in this

TABLE II.   The energies of the $cq\bar{q}\bar{q}$ system. $F_iS_jC_k$ stands for the index of flavor, spin, and color wave functions, respectively. E_{th} means the threshold of corresponding channel, E_{sc} is the energy of every single channel, E_{cc} shows the energy by channel coupling of one certain configuration, and E_{mix} is the lowest energy of the system by coupling all channels of both configurations. (unit: MeV).

IJ^P	$F_iS_jC_k$	Channel	E_{th}	E_{sc}	E_{cc}	E_{mix}	IJ^P	$F_iS_jC_k$	Channel	E_{th}	E_{sc}	E_{cc}	E_{mix}
$\frac{1}{2}0^+$	111	πD	2002	2004	2003	1998	$\frac{1}{2}1^+$	131	πD^*	2119	2121	2121	2120
	211	ηD	2532	2535				241	ωD	2564	2567		
	221	ωD^*	2682	2685				141	ρD	2635	2637		
	121	ρD^*	2753	2756				231	ηD^*	2650	2652		
								251	ωD^*	2682	2685		
								151	ρD^*	2753	2756		
	112	$[\pi]_8[D]_8$		2968				132	$[\omega]_8[D]_8$		2952		
	212	$[\eta]_8[D]_8$		3108				242	$[\rho]_8[D]_8$		2987		
	222	$[\omega]_8[D^*]_8$		2819				142	$[\pi]_8[D^*]_8$		2970		
	122	$[\rho]_8[D^*]_8$		2812				232	$[\eta]_8[D^*]_8$		3096		
								252	$[\omega]_8[D^*]_8$		2876		
								152	$[\rho]_8[D^*]_8$		2908		
	423	$[cq]_{\bar{3}}[\bar{q}\bar{q}]_3$		3037	2437			433	$[cq]_{\bar{3}}[\bar{q}\bar{q}]_3$		2955	2522	
	513	$[cq]_{\bar{3}}[\bar{q}\bar{q}]_3$		2514				543	$[cq]_{\bar{3}}[\bar{q}\bar{q}]_3$		2555		
	414	$[cq]_6[\bar{q}\bar{q}]_{\bar{6}}$		3054				453	$[cq]_{\bar{3}}[\bar{q}\bar{q}]_3$		3017		
	524	$[cq]_6[\bar{q}\bar{q}]_{\bar{6}}$		2854				534	$[cq]_6[\bar{q}\bar{q}]_{\bar{6}}$		3018		
								554	$[cq]_6[\bar{q}\bar{q}]_{\bar{6}}$		2935		
								444	$[cq]_6[\bar{q}\bar{q}]_{\bar{6}}$		3043		

IJ^P	$F_iS_jC_k$	Channel	E_{th}	E_{sc}	E_{cc}	E_{mix}	IJ^P	$F_iS_jC_k$	Channel	E_{th}	E_{sc}	E_{cc}	E_{mix}
$\frac{1}{2}2^+$	261	ωD^*	2682	2685	2685	2685	$\frac{3}{2}0^+$	311	πD	2002	2004	2004	2004
	161	ρD^*	2753	2755				321	ρD^*	2753	2756		
	262	$[\omega]_8[D]^*_8$		2999				312	$[\pi]_8[D]_8$		3018		
	162	$[\rho]_8[D^*]_8$		3059				322	$[\rho]_8[D^*]_8$		2918		
	463	$[cq]_{\bar{3}}[\bar{q}\bar{q}]_3$		2972	2972			623	$[cq]_{\bar{3}}[\bar{q}\bar{q}]_3$		3054	2838	
	564	$[cq]_6[\bar{q}\bar{q}]_{\bar{6}}$		3071				614	$[cq]_6[\bar{q}\bar{q}]_{\bar{6}}$		2903		

IJ^P	$F_iS_jC_k$	Channel	E_{th}	E_{sc}	E_{cc}	E_{mix}	IJ^P	$F_iS_jC_k$	Channel	E_{th}	E_{sc}	E_{cc}	E_{mix}
$\frac{3}{2}1^+$	331	πD^*	2119	2122	2122	2122	$\frac{3}{2}2^+$	361	ρD^*	2753	2756	2756	2756
	341	ρD	2635	2638									
	351	ρD^*	2753	2756									
	332	$[\pi]_8[D^*]_8$		2998									
	342	$[\rho]_8[D]_8$		3018				362	$[\rho]_8[D^*]_8$		3051		
	352	$[\rho]_8[D^*]_8$		2950									
	633	$[cq]_{\bar{3}}[\bar{q}\bar{q}]_3$		2952	2875			663	$[cq]_{\bar{3}}[\bar{q}\bar{q}]_3$		3036	3036	
	653	$[cq]_{\bar{3}}[\bar{q}\bar{q}]_3$		2955									
	644	$[cq]_6[\bar{q}\bar{q}]_{\bar{6}}$		3043									

work is lower than that in Ref. [76]. On the one hand, we add the Goldstone boson exchange interaction terms, which provide attractive interactions in the cq-$\bar{q}\bar{q}$ system. On the other hand, the lowest energy of this system is obtained by coupling four channels, as listed in Table II, while in Ref. [76], the minimum energy is obtained by coupling two channels, which are $|[nn]_0^{\bar{3}}(\bar{n}\bar{c}_0^3)\rangle_0$ and $|[nn]_1^6(\bar{n}\bar{c}_1^6)\rangle_0$.

Then, the channel coupling is calculated for all the twelve channels and the energy of 1988 MeV is obtained, which is 4 MeV lower than the minimum threshold (2002 MeV). This means channel-coupling effects are important for the formation of bound states. Besides, we also calculate the contributions of each term in the Hamilton and the root-mean-square (rms) distances in the $IJ^P = \frac{1}{2}0^+$ system,

which are listed in Table III. The energy contribution values in the table come from the difference between the contribution of each term in the tetraquark system and the sum of its contributions in the two individual mesons. From Table III, we can see that the kinetic and η-meson exchange terms provide repulsive interactions while the other terms provide attractive interactions. However, the attractive contribution is larger than the repulsive one, which provides the conditions for the $IJ^P = \frac{1}{2}0^+$ system to form a bound state. Moreover, for the bound state at the energy 1998 MeV, we label the quarks sequentially as 1, 2, 3, 4 (see Fig. 1). Since quarks 2 and 4 are identical particles, we cannot identify them. Therefore, for r_{12} and r_{14}, we obtained the same rms values. In fact, this value is the average of the c

TABLE III. Contributions of all potentials to the binding energy (unit: MeV) and root-mean-square distances (unit: fm) in the $cq\bar{q}\bar{q}$ system.

IJ^P	Energy	Kinetic	Conf	OGE	π	η	σ	B.E	r_{12}	r_{13}	r_{14}	r_{23}	r_{24}	r_{34}
$\frac{1}{2}0^+$	1998	50.8	−1.9	−13.6	−23.4	1.0	−16.9	−4	1.83	2.52	1.83	1.85	2.56	1.85

quark and two $\bar{q}$ quarks. The rms between the $\bar{q}$ and $\bar{q}$ quarks (r_{24}) in the tetraquark is 2.56 fm and the mean value for the q and $\bar{q}$ (r_{23} or r_{34}) is 1.85 fm. Using a triangular approximation ($r_{34}^2 = (r_{re}^2 + r_{24}^2)/2$), where r_{re} is the real rms of r_{34}, we can obtain a cluster of one meson ($q\bar{q}$) with a distance of about 0.54 fm, which is close to the rms we calculated for this meson alone. In the same way, the real rms of $c\bar{q}$ meson is about 0.38 fm. Thus, the distance between two quarks from different clumps is larger than 2 fm but the rms within the same cluster is around 0.5 fm, suggesting that the two clumps are separated by a wide distance. Moreover, we can see from the composition that the main component of this bound state is the $D\pi$ (98%) molecular state. From these two aspects, we propose the bound state dominated by the molecular structure.

In order to study the effect of the cutoff on the binding energy, we take different cutoffs to calculate the change in the binding energy. Firstly, we fix the cutoff of $\Lambda_\eta = 5.2$ fm^{-1} and gradually decrease the values of Λ_π and Λ_σ from 5.768 fm^{-1} to 2.16 fm^{-1}. When $\Lambda_\pi = \Lambda_\sigma = 3.5$ fm^{-1}, the binding energy of $cq\bar{q}\bar{q}$ with $IJ^P = 1/20^+$ is less than 1 MeV. When Λ_π, Λ_σ continues to decrease, this system changes from a bound state to a scattering state. For a fixed value of $\Lambda_\pi = \Lambda_\sigma = 4.2$ fm^{-1}, the cut-off value of Λ_η decreases from 5.768 fm^{-1} to 2.16 fm^{-1}. The binding energy keeps increasing, reaching about 5 MeV at $\Lambda_\eta = 2.16$ fm^{-1}. As can be seen from the above results, the binding energy is relatively sensitive to the cutoff. Actually, we generally treat these cut-off values as fixed and the cut-off values are from Ref. [77].

For the $IJ^P = \frac{1}{2}1^+$ system, the energy of each single channel is higher than the corresponding threshold. $c\bar{q}$-$q\bar{q}$ structure and cq-$\bar{q}\bar{q}$ structure are coupled separately, and the energies of both structures are 2121 and 2522 MeV, which are above the minimum threshold (2119 MeV). Then, channel coupling of two structures has been performed and the energy $E_{\text{mix}} = 2120$ MeV is obtained, which is still higher than the threshold. Therefore, no bound state below the minimum threshold is found for the $IJ^P = 01^+$ system.

For the $IJ^P = \frac{1}{2}2^+$ and $IJ^P = \frac{3}{2}0^+$ systems, both of them have four $c\bar{q}$-$q\bar{q}$ channels and two cq-$\bar{q}\bar{q}$ channels. Neither the single channel nor the channel-coupling energies are below the corresponding threshold. Therefore, for both systems, no bound states below the minimum threshold exist.

For the $IJ^P = \frac{3}{2}1^+$ system, there are nine channels, of which three are color-singlet, three are color-octet, and the remaining three are diquark-antidiquark channels. The single-channel and the channel-coupling calculations tell us that no bound states fall below the minimum threshold.

For the $IJ^P = \frac{3}{2}2^+$ system, the energy of each single channel is above the threshold of the ρD^*. The channel coupling cannot help too much. So there is no bound state below the threshold (2753 MeV) for this system, either.

According to the above discussion, there is only one bound state with the binding energy −4 MeV for the $IJ^P = \frac{1}{2}0^+$ in the $cq\bar{q}\bar{q}$ system. However, it is possible for the hidden-color channels to be resonance states, because the colorful subclusters cannot fall apart directly due to the color confinement. To check the possibility, we carry out a stabilization method, also named as a real-scaling method, which has proven to be a valuable tool for estimating the metastable energies of electron-atom, electron-molecule, and atom-diatom complexes [78].

In this approach, a factor α is used to scale the finite volume. As α increases, the false resonances will decay into the corresponding threshold channels, while the genuine resonances repeatedly appear as avoid-crossing structure (as shown in Fig. 2). This method has been successfully applied to the tetraquark system [56], petaquark system [79], and so on. It is important to note that for a genuine resonance state, its avoid-crossing structure is formed by a resonance line and a scattering line. However, if there are a large number of coupled channels, the avoid-crossing
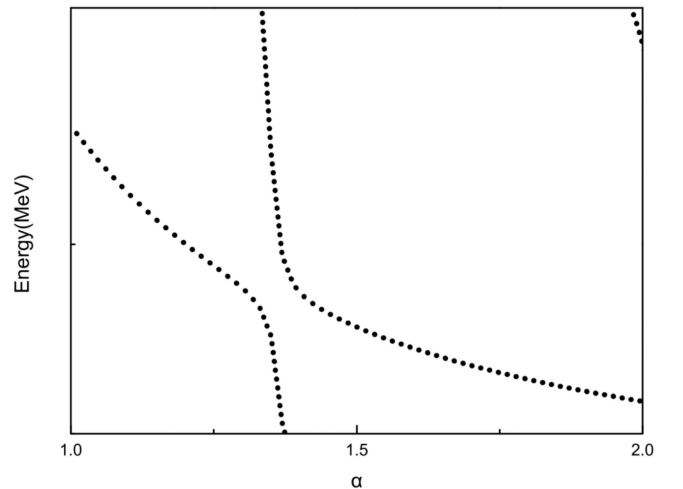
FIG. 2. The shape of the resonance in the real-scaling method. Taken from Ref. [78].
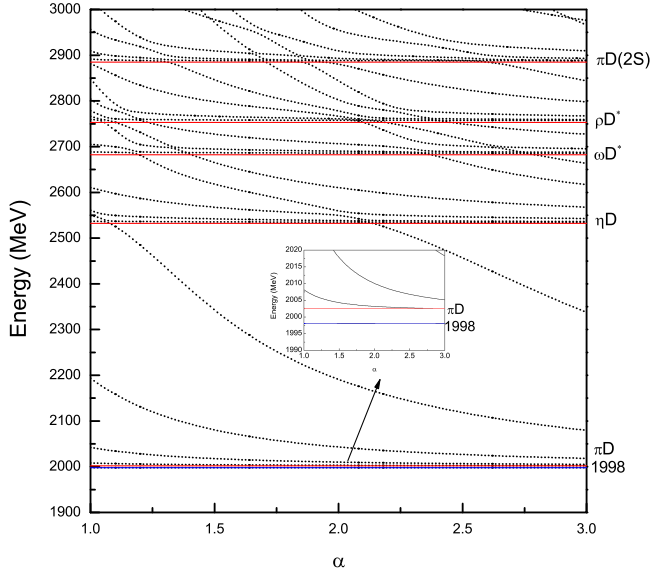
FIG. 3. The stabilization plots of the energies of the $cq\bar{q}\bar{q}$ system with $IJ^P = \frac{1}{2}0^+$.

structure is also formed due to the different rates of the scattering channel descending to the threshold line. We can further estimate whether it is a genuine resonance state by calculating the rms radius. It is important to note that for scattering states it is not square integrable in infinite space, but our calculations are performed in finite space, so a rms distance can be obtained. However, the rms distance of the scattering state will change with increasing space, while the rms distance of the resonance state will remain constant. By calculating the rms distance and the composition, we can
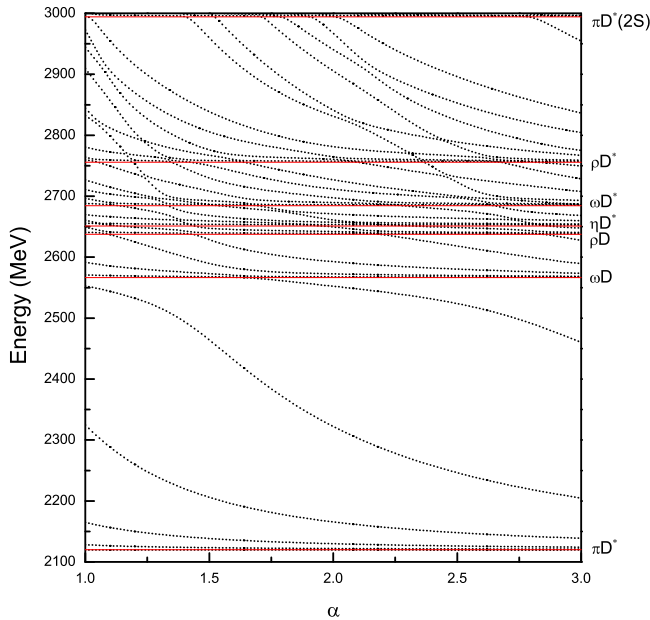
estimate whether the avoid-crossing structure is a genuine resonance state.

In this work, the value of α ranges from 1 to 3 to see if there is any resonance state. The results of the $cq\bar{q}\bar{q}$ tetraquark systems with $IJ^P = \frac{1}{2}0^+, \frac{1}{2}1^+, \frac{1}{2}2^+, \frac{3}{2}0^+, \frac{3}{2}1^+, \frac{3}{2}2^+$ are shown in Figs. 3–8, respectively. We mark the threshold in the red horizontal line and the genuine resonance state or a bound state in the blue horizontal line.

For the $cq\bar{q}\bar{q}$ system with $IJ^P = \frac{1}{2}0^+$ in Fig. 3, it is clear that the red horizontal lines located at the corresponding physical threshold of five channels πD, ηD, ωD^*, ρD^*, and $\pi D(2S)$. The blue horizontal line is the bound state at the energy 1998 MeV. Near energies 2780 MeV and 2926 MeV, the avoid-crossing structure is repeated. However, their main components are scattering states (more than 80%) and the rms distance will be larger than 6 fm with the expansion of space. So, we conclude that both of them are false resonance states. In this way, there is no resonance state for this system.

For the $IJ^P = \frac{1}{2}1^+$ system, in Fig. 4, seven red horizontal lines from bottom to top represent the thresholds of channels πD^*, ωD, ρD, ηD^*, ωD^*, ρD^*, and $\pi D^*(2S)$, respectively. The situation is similar to $IJ^P = \frac{1}{2}0^+$ system, so there is no genuine resonance state in this system.

For the $IJ^P = \frac{1}{2}2^+$ system, in Fig. 5, two red horizontal lines represent the thresholds of channels ωD^* and ρD, respectively. It is clear that as the α increases, the energy of the continuum state falls towards its threshold. So, there is no resonance state for this system.

For the $IJ^P = \frac{3}{2}0^+$ system, in Fig. 6, the thresholds of channels πD, ρD^*, and $\pi D(2S)$ are marked with red horizontal lines. In the vicinity of energies 2800 MeV

FIG. 4. The stabilization plots of the energies of the $cq\bar{q}\bar{q}$ system with $IJ^P = \frac{1}{2}1^+$.
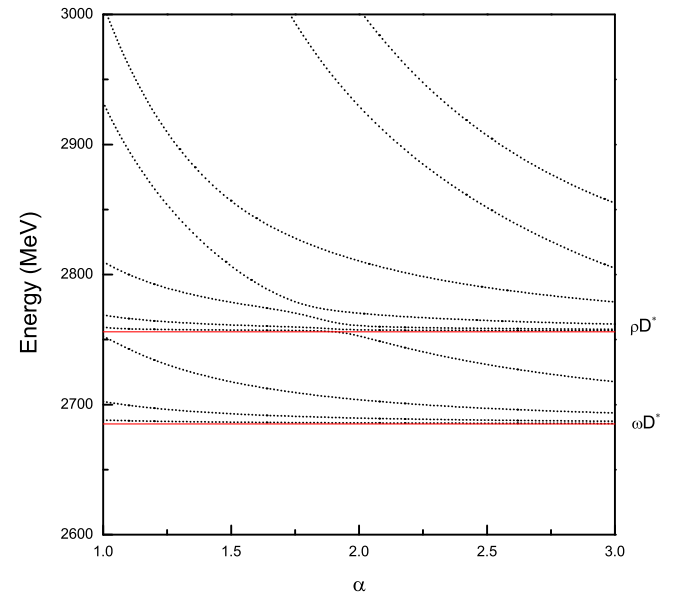
FIG. 5. The stabilization plots of the energies of the $cq\bar{q}\bar{q}$ system with $IJ^P = \frac{1}{2}2^+$.
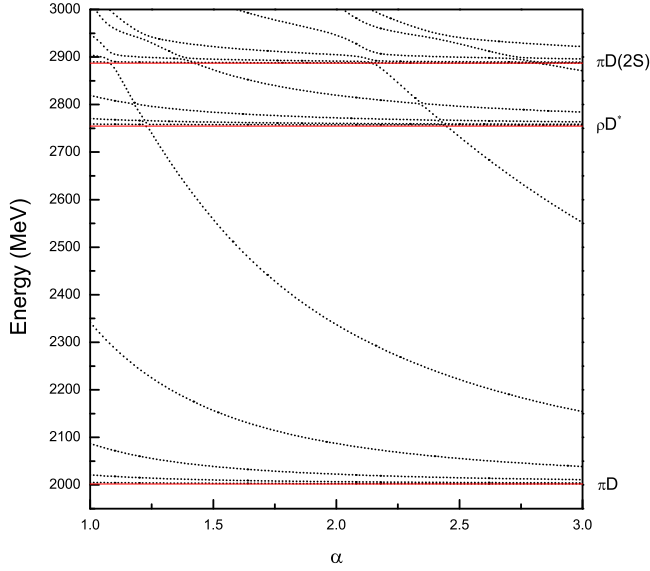
FIG. 6. The stabilization plots of the energies of the $cq\bar{q}\bar{q}$ system with $IJ^P = \frac{3}{2}0^+$.

and 2950 MeV, the scattering state composition exceeds 95% and 70%, respectively. Moreover, their rms distances are larger than 6 fm with the expansion of space, so that both of them are false resonance states. Therefore, there is no resonance state in this system.

For the $IJ^P = \frac{3}{2}1^+$ system, in Fig. 7, the thresholds of channels πD^*, ρD, ρD^*, and $\pi D^*(2S)$ are marked with red horizontal lines. Around the energy 2673 MeV and 2800 MeV, there are avoid-crossing structures. However, their rms distances are also unstable with increasing space, and their main components are also scattering states (around 93% and 86%, respectively), thus both of them
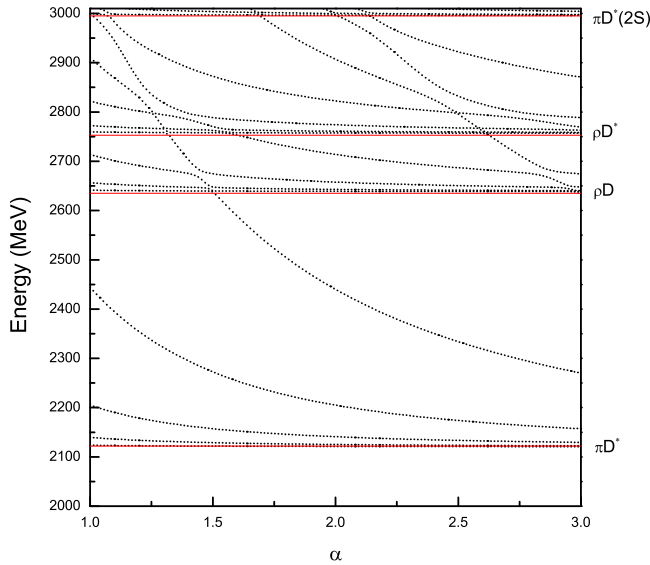
FIG. 7. The stabilization plots of the energies of the $cq\bar{q}\bar{q}$ system with $IJ^P = \frac{3}{2}1^+$.
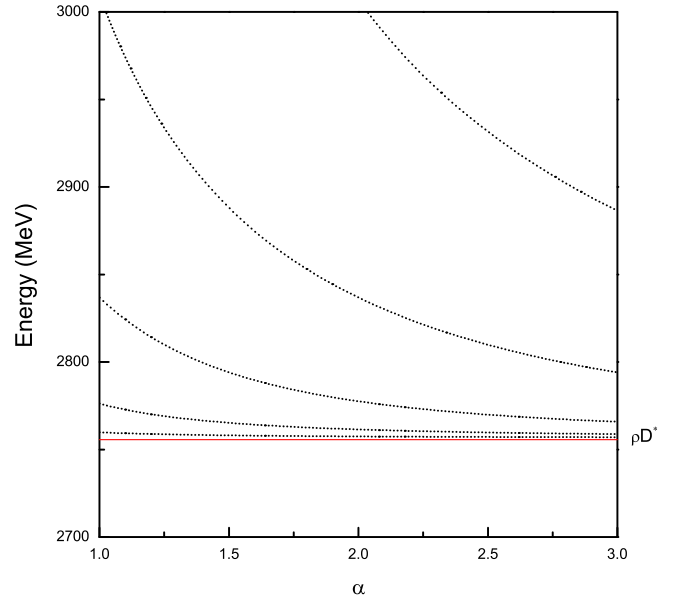
FIG. 8. The stabilization plots of the energies of the $cq\bar{q}\bar{q}$ system with $IJ^P = \frac{3}{2}2^+$.

are false resonance states. Therefore, there are also no resonance states in this system.

For the $IJ^P = \frac{3}{2}2^+$ system, in Fig. 8, the red horizontal line represents the threshold of the channel ρD^*. The case is similar to the $IJ^P = \frac{1}{2}2^+$ system, so there is no resonance state in the $IJ^P = \frac{3}{2}1^+$ system.

B. $bq\bar{q}\bar{q}$ system

The energies of the $bq\bar{q}\bar{q}$ tetraquark system are listed in Table IV. Meson-meson structure, diquark-antidiquark structure, and channel-coupling of two configurations are considered. Here, we also focus on the S-wave state. So, the possible quantum numbers are the same as the $cq\bar{q}\bar{q}$ system. Since the specific analysis is similar to that of the $cq\bar{q}\bar{q}$ system, to save space, we only give a brief description of the results for the $bq\bar{q}\bar{q}$ system.

From the numerical results in Table IV, we can see that for the $b\bar{q}$-$q\bar{q}$ system, there is no bound state below the minimum corresponding threshold for the single channel. However, after channel-coupling calculation, we obtain two bound states with binding energies −5 MeV in the $IJ^P = \frac{1}{2}1^+$ system and −2 MeV in the $IJ^P = \frac{1}{2}1^+$ system, respectively. Moreover, we also calculate the contributions of each term in the Hamilton and the rms distances in the $IJ^P = \frac{1}{2}0^+$ and $IJ^P = \frac{1}{2}1^+$ systems, respectively, listed in Table V. From Table V, we can see that for the $IJ^P = \frac{1}{2}0^+$ system with the energy of 5414 MeV, the confinement, OGE, π-meson exchange, and σ-meson exchange terms provide attractive interactions, while the kinetic term provide the repulsive interaction. The attraction provided

TABLE IV. The energies of the $bq\bar q\bar q$ system. $F_iS_jC_k$ stands for the index of flavor, spin, and color wave functions, respectively. E_{th} means the threshold of corresponding channel, E_{sc} is the energy of every single channel, E_{cc} shows the energy by channel coupling of one certain configuration, and E_{mix} is the lowest energy of the system by coupling all channels of both configurations. (unit: MeV).

IJ^P	$F_iS_jC_k$	Channel	E_{th}	E_{sc}	E_{cc}	E_{mix}	IJ^P	$F_iS_jC_k$	Channel	E_{th}	E_{sc}	E_{cc}	E_{mix}
$\frac{1}{2}0^+$	111	πB	5419	5421	5420	5414	$\frac{1}{2}1^+$	131	πB^*	5458	5460	5459	5456
	211	ηB	5950	5952				241	ωB	5982	5985		
	221	ωB^*	6021	6023				141	ρB	6053	6055		
	121	ρB^*	6092	6094				231	ηB^*	5989	5991		
								251	ωB^*	6021	6023		
								151	ρB^*	6092	6094		
	112	$[\pi]_8[B]_8$		6327				132	$[\omega]_8[B]_8$		6310		
	212	$[\eta]_8[B]_8$		6465				242	$[\rho]_8[B]_8$		6342		
	222	$[\omega]_8[B^*]_8$		6207				142	$[\pi]_8[B^*]_8$		6328		
	122	$[\rho]_8[B^*]_8$		6213				232	$[\eta]_8[B^*]_8$		6461		
								252	$[\omega]_8[B^*]_8$		6258		
								152	$[\rho]_8[B^*]_8$		6279		
	423	$[bq]_{\bar3}[\bar q\bar q]_3$		6383	5828			433	$[bq]_{\bar3}[\bar q\bar q]_3$		6318	5858	
	513	$[bq]_{\bar3}[\bar q\bar q]_3$		5877				543	$[bq]_{\bar3}[\bar q\bar q]_3$		5892		
	414	$[bq]_6[\bar q\bar q]_{\bar6}$		6415				453	$[bq]_{\bar3}[\bar q\bar q]_3$		6359		
	524	$[bq]_6[\bar q\bar q]_{\bar6}$		6256				534	$[bq]_6[\bar q\bar q]_{\bar6}$		6378		
								554	$[bq]_6[\bar q\bar q]_{\bar6}$		6317		
								444	$[bq]_6[\bar q\bar q]_{\bar6}$		6410		

IJ^P	$F_iS_jC_k$	Channel	E_{th}	E_{sc}	E_{cc}	E_{mix}	IJ^P	$F_iS_jC_k$	Channel	E_{th}	E_{sc}	E_{cc}	E_{mix}
$\frac{1}{2}2^+$	261	ωB^*	6021	6024	6024	6024	$\frac{3}{2}0^+$	311	πB	5419	5422	5422	5422
	161	ρB^*	6092	6093				321	ρB^*	6092	6094		
	262	$[\omega]_8[B]_8^*$		6345				312	$[\pi]_8[B]_8$		6371		
	162	$[\rho]_8[B^*]_8$		6406				322	$[\rho]_8[B^*]_8$		6296		
	463	$[bq]_{\bar3}[\bar q\bar q]_3$		6305	6305			623	$[bq]_{\bar3}[\bar q\bar q]_3$		6252	6208	
	564	$[bq]_6[\bar q\bar q]_{\bar6}$		6424				614	$[bq]_6[\bar q\bar q]_{\bar6}$		6415		

IJ^P	$F_iS_jC_k$	Channel	E_{th}	E_{sc}	E_{cc}	E_{mix}	IJ^P	$F_iS_jC_k$	Channel	E_{th}	E_{sc}	E_{cc}	E_{mix}
$\frac{3}{2}1^+$	331	πB^*	5458	5461	5461	5461	$\frac{3}{2}2^+$	361	ρB^*	6092	6095	6095	6095
	341	ρB	6053	6056									
	351	ρB^*	6092	6094									
	332	$[\pi]_8[B^*]_8$		6363				362	$[\rho]_8[B^*]_8$		6404		
	342	$[\rho]_8[B]_8$		6379									
	352	$[\rho]_8[B^*]_8$		6335									
	633	$[bq]_{\bar3}[\bar q\bar q]_3$		6294	6222			663	$[bq]_{\bar3}[\bar q\bar q]_3$		6369	6369	
	653	$[bq]_{\bar3}[\bar q\bar q]_3$		6318									
	644	$[bq]_6[\bar q\bar q]_{\bar6}$		6410									

by the π-meson exchange and σ-meson exchange counteracts most of the repulsion from the kinetic term. So, the contributions of Goldstone boson exchanges play an important role in the formation of the bound states. Moreover, the rms distances among the quarks are 1.6–2.2 fm and the main component of this bound state is πB (97%), which indicates that this bound state is dominated by the molecular structure. The situation is similar for the $IJ^P = \frac{1}{2}1^+$ system. The lowest energy is 5456 MeV with the main component of πB^* (98%), and the rms distances among the quarks are 1.8–2.6 fm, also showing that this bound state is dominated by the molecular structure. Besides, the real-scaling method is also employed to search for resonance states in

TABLE V. Contributions of all potentials to the binding energy (unit: MeV) and root-mean-square distances (unit: fm) in the $bq\bar q\bar q$ system.

IJ^P	Energy	Kinetic	Conf	OGE	π	η	σ	B.E	r_{12}	r_{13}	r_{14}	r_{23}	r_{24}	r_{34}
$\frac{1}{2}0^+$	5414	48.0	-2.6	-8.4	-25.2	0.9	-17.7	-5	1.61	2.18	1.61	1.64	2.25	1.64
$\frac{1}{2}1^+$	5456	34.5	-1.9	-2.9	-19.6	0.6	-14.0	-2	1.86	2.56	1.86	1.89	2.62	1.89
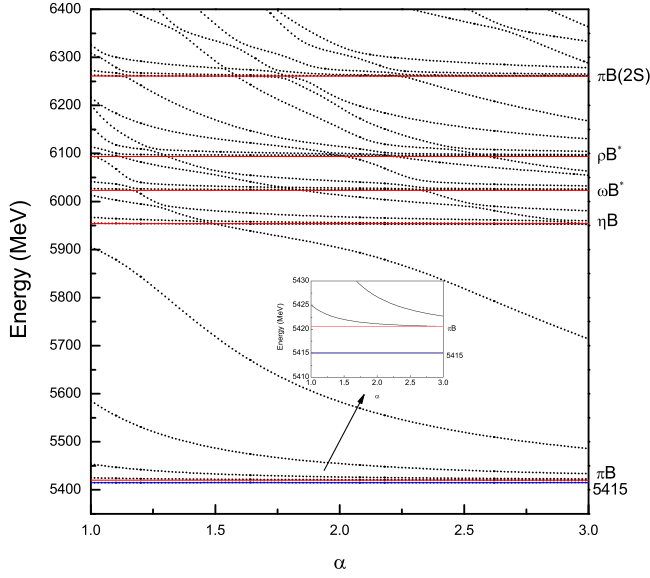
FIG. 9. The stabilization plots of the energies of the $bq\bar{q}\bar{q}$ system with $IJ^P = \frac{1}{2}0^+$.

FIG. 11. The stabilization plots of the energies of the $bq\bar{q}\bar{q}$ system with $IJ^P = \frac{1}{2}2^+$.

the $bq\bar{q}\bar{q}$ system. The results are shown in Figs. 9–14, which show that there is no any genuine resonance state in the $bq\bar{q}\bar{q}$ system.

For both bound states in the $bq\bar{q}\bar{q}$ system, we also investigate the effect of the cutoff on the binding energies. The general trend is the same as for the $cq\bar{q}\bar{q}$ system. The difference, however, is that as the cutoff is varied, with the binding energy with $IJ^P = 1/20^+$ being as high as -6 MeV and the binding energy with $IJ^P = 1/21^+$ up to -3 MeV.
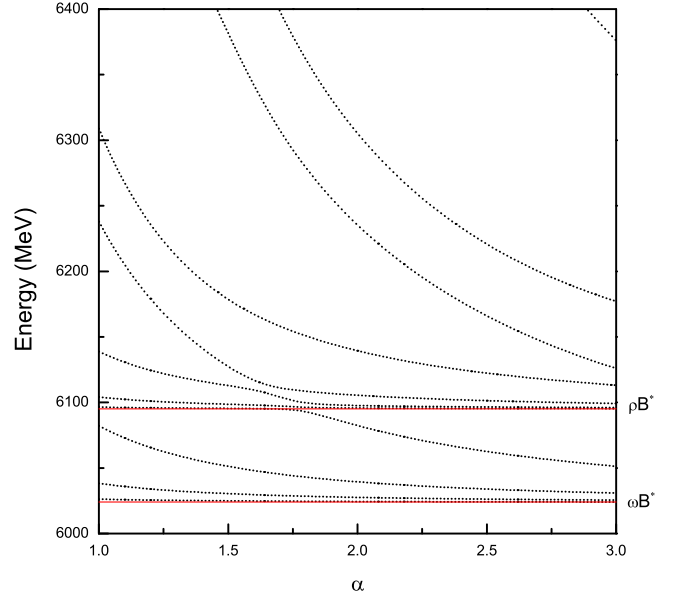
IV. SUMMARY

In this work, the low-lying system $Qq\bar{q}\bar{q}$ ($Q = c$, b and $q = u, d$) is systematically investigated in the framework of the ChQM. $Q\bar{q}$-$q\bar{q}$, Qq-$\bar{q}\bar{q}$ structures, and channel coupling of these two configurations are considered. In order to search for the bound state in the $Qq\bar{q}\bar{q}$ system, dynamical bound-state calculations have been performed. At the same time, a real-scaling method is employed to find the genuine resonance states.

FIG. 10. The stabilization plots of the energies of the $bq\bar{q}\bar{q}$ system with $IJ^P = \frac{1}{2}1^+$.
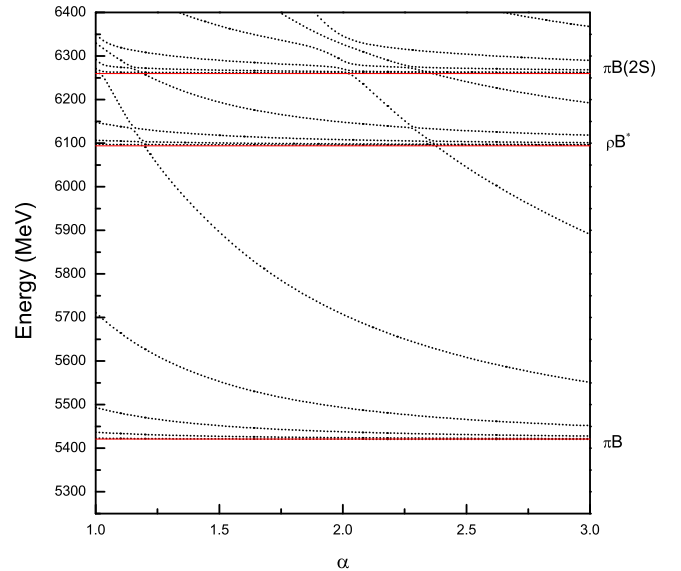
FIG. 12. The stabilization plots of the energies of the $bq\bar{q}\bar{q}$ system with $IJ^P = \frac{3}{2}0^+$.
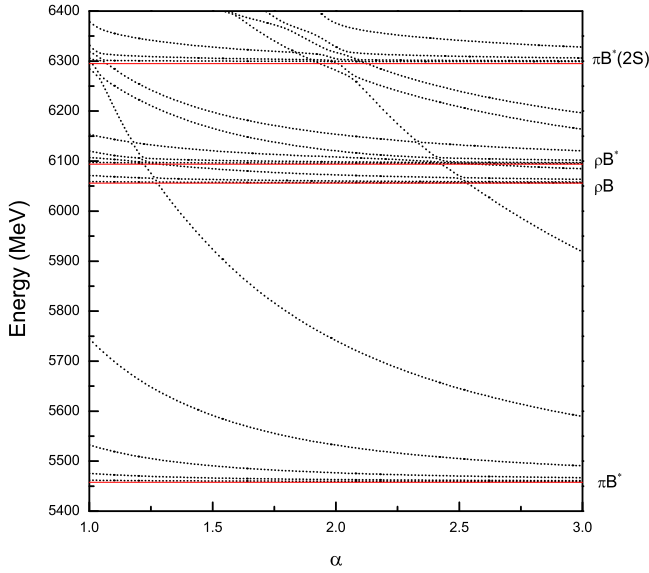
FIG. 13. The stabilization plots of the energies of the $bq\bar{q}\bar{q}$ system with $IJ^P = \frac{3}{2}1^+$.

The bound-state calculations show that for the single channel, there is no evidence for any bound state below the minimum threshold in both $cq\bar{q}\bar{q}$ and $bq\bar{q}\bar{q}$ systems. However, after coupling all channels, we obtain a bound state below the minimum threshold in the $cq\bar{q}\bar{q}$ system with the binding energy of 4 MeV, and the quantum number is $IJ^P = \frac{1}{2}0^+$. Meanwhile, in the $bq\bar{q}\bar{q}$ system, two bound states with binding energies of 5 MeV and 2 MeV are obtained, and the quantum numbers are $IJ^P = \frac{1}{2}0^+$ and $IJ^P = \frac{1}{2}1^+$, respectively. All three bound states are obtained by channel coupling, suggesting that channel
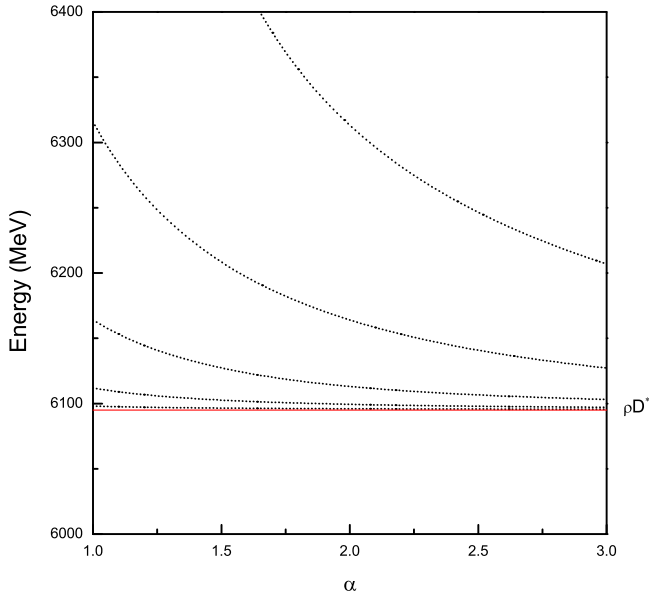
FIG. 14. The stabilization plots of the energies of the $bq\bar{q}\bar{q}$ system with $IJ^P = \frac{3}{2}2^+$.

coupling effects are important for the formation of bound states. Moreover, for these three bound states, we study the contributions of each term in Hamiltonian, and the results indicate that the Goldstone boson exchange contributions play a dominant role in the formation of bound states in the $Qq\bar{q}\bar{q}$ ($Q = c$, b and $q = u$, d) system. To investigate the structure of the bound states, we also calculate the rms distances between quarks and the channel components of the bound states. The results show that all of the bound states are dominated by the molecular structure.

To study the dependence of the cutoff on the bound state, we adjust different cut-off values to observe the change in the binding energy. When we fix the value of $\Lambda_\eta = 5.2$ fm^{-1}, we find that at $\Lambda_\pi = \Lambda_\sigma = 3.5$ fm^{-1}, the binding energy is less than 1 MeV. As we continue to decrease the values of Λ_π and Λ_σ, the binding energy vanishes. When the values of $\Lambda_\pi = \Lambda_\sigma$ are 3.5 fm^{-1}, the binding energy will increase about 2–3 MeV. From the numerical results we can see that the binding energy is relatively sensitive to the cutoff.

Besides, this work shows that the coupling of various configurations is important to search for resonance states. We consider not only the cq-$\bar{q}\bar{q}$ structure, but also the $c\bar{q}$-$q\bar{q}$ structure and the channel coupling of the two configurations. It is known that cq-$\bar{q}\bar{q}$ states are possible resonance states, but they could be coupled to the $c\bar{q}$-$q\bar{q}$ states, such that the cq-$\bar{q}\bar{q}$ states may decay to the corresponding threshold. We can estimate whether a resonance state exists after coupling the two structure by employing the real-scaling method. After calculations and analysis with the real-scaling method, we find that the cq-$\bar{q}\bar{q}$ states decay to the corresponding threshold. So, there is no genuine resonance state in $cq\bar{q}\bar{q}$ and $bq\bar{q}\bar{q}$ systems in present work.

It is worth noting that the lowest-lying positive-parity charmed mesons, which are directly related to the tetraquark states here, need to be discussed. The lightest charmed scalar meson with positive parity is known as $D_0^*(2300)$ observed at Belle Collaboration [80]. In Ref. [81], the authors show that the parameters assigned to the lightest scalar D meson are in conflict with the precise LHCb data of the decay $B^- \to D^+\pi^-\pi^-$ [82] and these data can be well reproduced by the unitarized chiral perturbation theory amplitude containing the $D_0^*(2100)$. The lowest $D_0^*(2100)$ is close to our binding energy (1998) in the $cq\bar{q}\bar{q}$ tetraquark system with $IJ^P = 1/20^+$. Therefore, we calculate the P-wave $IJ^P = 1/20^+$ scalar D meson. Its mass is 2454 MeV, which is much higher than the binding energy (1998 MeV) of the $cq\bar{q}\bar{q}$ system. Thus, we expect that the mixing of P-wave meson with tetraquark in the $IJ^P = 1/20^+$ state will not affect the result much. For the $bq\bar{q}\bar{q}$ with $IJ^P = 1/20^+$ and $IJ^P = 1/21^+$ systems, the situation is similar to the $cq\bar{q}\bar{q}$ system. For the bound states, we can via possible decay process to

reconstruct them, using scattering phase shifts or correlation functions, and thus confirm whether the bound states exist or not.Take bound state 1998 [X(1998)], for example. In the $cq\bar{q}\bar{q}$ system with $IJ^P = 1/20^+$ state, through the process $X(1998) \to K_S\pi\pi$, the experiment can measure the final state particles, reconstruct $X(1998)$ from this information, and thus find out whether $X(1998)$ exists or not. In the same way, for the bound state 5414[X(5414)] with $IJ^P = 1/20^+$ state in the $bq\bar{q}\bar{q}$ system, one can utilize decay process $X(5414) \to D^*K^*\pi$ to reconstruct $X(5414)$, and determine its existence. Regarding the bound state 5456[X(5456)]

with $IJ^P = 1/21^+$ state, the decay process $X(5456) \to D\pi\pi$ can be employed to reconstruct $X(5456)$, which makes it easier to determine its existence.

[1] R. Aaij *et al.* (LHCb Collaboration), Nat. Commun. **13,** 3351 (2022).

[2] S. K. Choi *et al.* (Belle Collaboration), Phys. Rev. Lett. **91,** 262001 (2003).

[3] R. Aaij *et al.* (LHCb Collaboration), Phys. Rev. Lett. **131,** 071901 (2023).

[4] R. Aaij *et al.* (LHCb Collaboration), Phys. Rev. Lett. **115,** 072001 (2015).

[5] V. M. Abazov *et al.* (D0 Collaboration), Phys. Rev. Lett. **117,** 022003 (2016).

[6] R. Aaij *et al.* (LHCb Collaboration), Phys. Rev. Lett. **117,** 152003 (2016).

[7] T. Aaltonen *et al.* (CDF Collaboration), Phys. Rev. Lett. **120,** 202006 (2018).

[8] A. M. Sirunyan *et al.* (CMS Collaboration), Phys. Rev. Lett. **120,** 202005 (2018).

[9] M. Aaboud *et al.* (ATLAS Collaboration), Phys. Rev. Lett. **120,** 202007 (2018).

[10] C. M. Zanetti, M. Nielsen, and K. P. Khemchandani, Phys. Rev. D **93,** 096011 (2016).

[11] W. Chen, H. X. Chen, X. Liu, T. G. Steele, and S. L. Zhu, Phys. Rev. Lett. **117,** 022002 (2016).

[12] Z. G. Wang, Commun. Theor. Phys. **66,** 335 (2016).

[13] S. S. Agaev, K. Azizi, and H. Sundu, Phys. Rev. D **93,** 094006 (2016).

[14] X. H. Liu and G. Li, Eur. Phys. J. C **76,** 455 (2016).

[15] W. Wang and R. Zhu, Chin. Phys. C **40,** 093101 (2016).

[16] Z. G. Wang, Eur. Phys. J. C **76,** 279 (2016).

[17] S. S. Agaev, K. Azizi, and H. Sundu, Phys. Rev. D **93,** 114007 (2016).

[18] J. M. Dias, K. P. Khemchandani, A. Martínez Torres, M. Nielsen, and C. M. Zanetti, Phys. Lett. B **758,** 235 (2016).

[19] F. Goerke, T. Gutsche, M. A. Ivanov, J. G. Korner, V. E. Lyubovitskij, and P. Santorelli, Phys. Rev. D **94,** 094017 (2016).

[20] H. Huang and J. Ping, Eur. Phys. J. C **79,** 556 (2019).

[21] F. K. Guo, U. G. Meißner, and B. S. Zou, Commun. Theor. Phys. **65,** 593 (2016).

[22] M. Albaladejo, J. Nieves, E. Oset, Z. F. Sun, and X. Liu, Phys. Lett. B **757,** 515 (2016).

[23] X. Chen and J. Ping, Eur. Phys. J. C **76,** 351 (2016).

[24] C. B. Lang, D. Mohler, and S. Prelovsek, Phys. Rev. D **94,** 074509 (2016).

[25] R. Chen and X. Liu, Phys. Rev. D **94,** 034006 (2016).

[26] R. Aaij *et al.* (LHCb Collaboration), Phys. Rev. Lett. **125,** 242001 (2020).

[27] R. Aaij *et al.* (LHCb Collaboration), Phys. Rev. D **102,** 112003 (2020).

[28] R. Molina, T. Branz, and E. Oset, Phys. Rev. D **82,** 014010 (2010).

[29] R. Molina and E. Oset, Phys. Lett. B **811,** 135870 (2020).

[30] Y. Xue, X. Jin, H. Huang, and J. Ping, Phys. Rev. D **103,** 054010 (2021).

[31] S. S. Agaev, K. Azizi, and H. Sundu, J. Phys. G **48,** 085012 (2021).

[32] J. He and D. Y. Chen, Chin. Phys. C **45,** 063102 (2021).

[33] C. J. Xiao, D. Y. Chen, Y. B. Dong, and G. W. Meng, Phys. Rev. D **103,** 034004 (2021).

[34] M. Karliner and J. L. Rosner, Phys. Rev. D **102,** 094016 (2020).

[35] Z. G. Wang, Int. J. Mod. Phys. A **35,** 2050187 (2020).

[36] Y. Tan and J. Ping, Chin. Phys. C **45,** 093104 (2021).

[37] Y. Huang, J. X. Lu, J. J. Xie, and L. S. Geng, Eur. Phys. J. C **80,** 973 (2020).

[38] H. X. Chen, W. Chen, R. R. Dong, and N. Su, Chin. Phys. Lett. **37,** 101201 (2020).

[39] J. R. Zhang, Phys. Rev. D **103,** 054019 (2021).

[40] Y. K. Chen, J. J. Han, Q. F. Lü, J. P. Wang, and F. S. Yu, Eur. Phys. J. C **81,** 71, (2021).

[41] T. J. Burns and E. S. Swanson, Phys. Rev. D **103,** 014004 (2021).

[42] R. Aaij *et al.* (LHCb Collaboration), Phys. Rev. Lett. **131,** 041902 (2023).

[43] S. S. Agaev, K. Azizi, and H. Sundu, J. Phys. G **50,** 055002 (2023).

[44] M. Y. Duan, M. L. Du, Z. H. Guo, E. Wang, and D. Y. Chen, Phys. Rev. D **108,** 074006 (2023).

[45] F. X. Liu, R. H. Ni, X. H. Zhong, and Q. Zhao, Phys. Rev. D **107,** 096020 (2023).

[46] J. Wei, Y. H. Wang, C. S. An, and C. R. Deng, Phys. Rev. D **106,** 096023 (2022).

[47] H. W. Ke, Y. F. Shi, X. H. Liu, and X. Q. Li, Phys. Rev. D **106**, 114032 (2022).

[48] Z. L. Yue, C. J. Xiao, and D. Y. Chen, Phys. Rev. D **107**, 034018 (2023).

[49] W. T. Lyu, Y. H. Lyu, M. Y. Duan, D. M. Li, D. Y. Chen, and E. Wang, Phys. Rev. D **109**, 014008 (2024).

[50] Y. Huang, H. Hei, J. w. Feng, X. Chen, and R. Wang, Phys. Rev. D **108**, 076019 (2023).

[51] M. Y. Duan, E. Wang, and D. Y. Chen, arXiv:2305.09436.

[52] K. G. Wilson, Phys. Rev. D **10**, 2445 (1974).

[53] F. Wang, G. h. Wu, L. j. Teng, and J. T. Goldman, Phys. Rev. Lett. **69**, 2901 (1992).

[54] V. A. Novikov, L. B. Okun, M. A. Shifman, A. I. Vainshtein, M. B. Voloshin, and V. I. Zakharov, Phys. Rev. Lett. **38**, 626 (1977).

[55] A. Valcarce, H. Garcilazo, F. Fernandez, and P. Gonzalez, Rep. Prog. Phys. **68**, 965 (2005).

[56] Y. Tan, X. Liu, X. Chen, H. Huang, and J. Ping, Phys. Rev. D **108**, 014017 (2023).

[57] X. Hu and J. Ping, Eur. Phys. J. C **82**, 118 (2022).

[58] M. Pan, X. Zhu, and J. Ping, Eur. Phys. J. C **83**, 645 (2023).

[59] E. Hiyama, Y. Kino, and M. Kamimura, Prog. Part. Nucl. Phys. **51**, 223 (2003).

[60] Y. Tan and J. Ping, Phys. Rev. D **100**, 034022 (2019).

[61] X. Hu and J. Ping, Phys. Rev. D **106**, 054028 (2022).

[62] G. Yang, J. Ping, and J. Segovia, Phys. Rev. D **104**, 014006 (2021).

[63] Y. Lu, M. N. Anwar, and B. S. Zou, Phys. Rev. D **94**, 034021 (2016).

[64] X. Chen and J. Ping, Phys. Rev. D **98**, 054022 (2018).

[65] Y. Yang, C. Deng, J. Ping, and T. Goldman, Phys. Rev. D **80**, 114023 (2009).

[66] J. Vijande, F. Fernandez, and A. Valcarce, J. Phys. G **31**, 481 (2005).

[67] A. Buchmann, E. Hernandez, and K. Yazaki, Phys. Lett. B **269**, 35 (1991).

[68] S. Godfrey and N. Isgur, Phys. Rev. D **32**, 189 (1985).

[69] R. L. Jaffe, Phys. Rev. D **15**, 267 (1977).

[70] J. R. Pelaez, Phys. Rep. **658**, 1 (2016).

[71] B. Wu, X. H. Cao, X. K. Dong, and F. K. Guo, Phys. Rev. D **109**, 034026 (2024).

[72] K. Brauer, A. Faessler, F. Fernandez, and K. Shimizu, Nucl. Phys. **A507**, 599 (1990).

[73] Z. Y. Zhang, A. Faessler, U. Straub, and L. Y. Glozman, Nucl. Phys. **A578**, 573 (1994).

[74] L. R. Dai, Z. Y. Zhang, Y. W. Yu, and S. L. Yuan, HEPNP **28**, 1324 (2004).

[75] Y. Tan, W. Lu, and J. Ping, Eur. Phys. J. Plus **135**, 716 (2020).

[76] Q. F. Lü, D. Y. Chen, and Y. B. Dong, Phys. Rev. D **102**, 074021 (2020).

[77] J. Vijande, F. Fernandez, and A. Valcarce, J. Phys. G **31**, 481 (2005).

[78] J. Simons, J. Chem. Phys. **75**, 2465 (1981).

[79] E. Hiyama, A. Hosaka, M. Oka, and J. M. Richard, Phys. Rev. C **98**, 045208 (2018).

[80] K. Abe *et al.* (Belle Collaboration), Phys. Rev. D **69**, 112002 (2004).

[81] M. L. Du, F. K. Guo, C. Hanhart, B. Kubis, and U. G. Meißner, Phys. Rev. Lett. **126**, 192001 (2021).

[82] R. Aaij *et al.* (LHCb Collaboration), Phys. Rev. D **94**, 072001 (2016).